# Outage Analysis of Multi-User Massive MIMO Systems Subject to Composite Fading

Muhammad Saad Zia and Syed Ali Hassan
School of Electrical Engineering and Computer Science (SEECS)
National University of Sciences and Technology (NUST), Islamabad, Pakistan
Email: {12mseemzia, ali.hassan} @seecs.edu.pk

***Abstract*—Multiple single antenna terminals transmit simultaneously to an array of hundreds of antennas in the uplink of a multi-user massive multiple-input-multiple-output (MIMO) system. Under Rayleigh fading and lognormal shadowing, the expression for the probability density function (PDF) for signal-to-interference-plus-noise-ratio (SINR) does not exist in a closed-form, which is required to calculate the outage probability of a user. This paper provides approximate closed-form expressions for the outage probability of a user when the base station (BS) uses a maximum-ratio-combining (MRC) receiver in the presence of above channel impairments. It has been shown that the PDF of SINR can be well-approximated by a lognormal random variable (RV). Moreover, the effects of shadowing on the performance of the system have been quantified and it has been shown that the shadowing does not average out by increasing the number of antennas.**

## I. Introduction

Massive multiple-input-multiple-output (MIMO) is a novel concept that uses hundreds of antennas at the base station (BS) to serve tens of users simultaneously in the same time-frequency resource [1], [2]. In massive MIMO systems, a large number of BS antennas improve spectral efficiency and radiated energy efficiency as compared to the existing wireless technologies. The excessive BS antennas make use of the concept of beamforming by transmitting only in the desired directions so that the radiated energy is focused in a small region and interference is minimized [3]– [4].

Multi-user massive MIMO systems allow an increase in the theoretical capacity and reduction in uplink (UL) and downlink (DL) power consumption [5]. Such systems allow the use of low cost hardware at the BS by reducing the peak-to-average-power-ratio (PAPR) in the downlink [6]. All these reasons make massive MIMO a viable solution for future broadband technologies. As the number of antennas at the BS increases, linear receivers such as maximum ratio combining (MRC) and minimum mean squared error (MMSE) become optimal.

With a large number of BS antennas, things that were random before, now start to look deterministic. As a consequence, thermal noise and small-scale fading are averaged out in massive MIMO systems. However, the effects of shadowing still remain. The shadowing in wireless systems is known to follow a lognormal distribution. Under Rayleigh fading and lognormal shadowing, the expressions for the probability density function (PDF) of signal-to-interference-plus-noise-ratio (SINR) for massive MIMO systems do not exist in a closed-form. Closed-form expressions for the PDF of SINR are needed to calculate the outage probability and capacity of the system.

In this paper, we analyze an MRC receiver for a massive MIMO system operating under a composite Rayleigh fading-lognormal shadowing channel. The analysis is divided into two steps. We first analyze the signal-to-noise-ratio (SNR) of a single user. We approximate the PDF of the SNR by a new lognormal random variable (RV) using two different methods namely, the moment matching (MM) method and the moment generating function (MGF)-based method. Using the SNR analysis, we formulate the SINR for a single user in a multi-user scenario. In the second step, we show that the SINR can also be approximated by a lognormal RV. The PDF of the new approximating lognormal RV is then used to calculate the outage probability of massive MIMO systems for varying channel parameters. We illustrate the effect of lognormal shadowing on the outage of these systems and prove that unlike small-scale fading, large-scale does not average out by increasing the number of BS antennas.

The next section gives the system model for a multi-user massive MIMO system under composite Rayleigh fading-lognormal shadowing environment. Lognormal approximations of SNR and SINR are given in sections III and IV, respectively. Numerical results and discussions follow in Section V. Finally, the conclusion and future work are given in Section VI.

## II. System Model

Consider the uplink of a single cell multi-user massive MIMO system with one BS equipped with $M$ antennas. The BS receives the data from $K$ single-antenna users, which is corrupted by the channel impairments. The transmissions from $K$ users to the BS suffer from independent Rayleigh fading and lognormal shadowing. The $M \times 1$ received signal vector at the BS is given by

$$\boldsymbol{y} = \sqrt{P_t}\boldsymbol{G}\boldsymbol{x} + \boldsymbol{n}, \tag{1}$$

where $\boldsymbol{G}$ represents the $M \times K$ channel matrix between the $K$ users and the $M$ BS antennas, $P_t$ is the average transmit power of a single user, $\boldsymbol{x}$ is the vector of symbols transmitted simultaneously by $K$ users and $\boldsymbol{n}$ is the noise vector.

The channel matrix $\boldsymbol{G}$ models Rayleigh fading and lognormal shadowing. The channel coefficient $g_{ik}$ between the $i$th

978-1-4799-8088-8/15/$31.00 ©2015 IEEE

BS antenna and the $k$th user can be represented as

$$g_{ik} = h_{ik}\sqrt{\nu_k}, \tag{2}$$

where $h_{ik}$ is the small-scale (Rayleigh) fading coefficient between the $i$th BS antenna and the $k$th user and $\nu_k$ represents the large-scale fading (lognormal shadowing) component of the $k$th user such that $h_{ik} \sim \mathcal{CN}(0,1)$, and $\nu_k = 10^{0.1X_k}$ where $X_k \sim \mathcal{N}(\mu_{(dB)}, \sigma^2_{(dB)})$. Since the BS antennas are closely spaced, the large-scale fading for a single user across $M$ BS antennas is correlated. However, the small-scale fading coefficients are independent and identically distributed (i.i.d). In this paper, we assume perfect correlation between the shadowing components of a single user across $M$ BS antennas. The channel matrix $\boldsymbol{G}$ is then given by

$$\boldsymbol{G} = \boldsymbol{H}\boldsymbol{V}^{1/2}, \tag{3}$$

where $\boldsymbol{H}$ is the $M \times K$ matrix of small-scale fading coefficients between the $M$ BS antennas and $K$ users and $\boldsymbol{V}$ is a $K \times K$ diagonal matrix containing the large-scale fading coefficients of $K$ users. By using a linear detector, the received signal $\boldsymbol{y}$ is processed as follows

$$\boldsymbol{r} = \boldsymbol{A}^H\boldsymbol{y}, \tag{4}$$

where $\boldsymbol{A}$ is the linear detector matrix that depends on the channel matrix $\boldsymbol{G}$ and $H$ is the Hermitian operator. After applying the linear detector, the received signal vector is given by

$$\boldsymbol{r} = \sqrt{P_t}\boldsymbol{A}^H\boldsymbol{G}\boldsymbol{x} + \boldsymbol{A}^H\boldsymbol{n}, \tag{5}$$

The vector $\boldsymbol{r}$ gives the received signals from all the users. Let $r_j$ and $x_j$ represent the received signal and the transmitted symbol of the $j$th user, respectively. Then

$$r_j = \sqrt{P_t}\boldsymbol{a}_j^H\boldsymbol{g}_j x_j + \sqrt{P_t}\sum_{k=1,k\neq j}^{K}\boldsymbol{a}_j^H\boldsymbol{g}_k x_k + \boldsymbol{a}_j^H\boldsymbol{n}, \tag{6}$$

where $\boldsymbol{a}_j$ and $\boldsymbol{g}_j$ represent the $j$th columns of the matrices $\boldsymbol{A}$ and $\boldsymbol{G}$, respectively. The first term in (6) gives the desired signal of the $j$th user whereas the other two terms constitute interference from other users and noise, respectively. Without loss of generality, we assume unit power spectral density of noise. The SINR of the $j$th user can then be represented as

$$SINR_j = \frac{P_t|\boldsymbol{a}_j^H\boldsymbol{g}_j|^2}{P_t\sum_{k=1,k\neq j}^{K}|\boldsymbol{a}_j^H\boldsymbol{g}_k|^2 + \|\boldsymbol{a}_j\|^2}. \tag{7}$$

In case of perfect channel state information (CSI) and MRC, $\boldsymbol{A} = \boldsymbol{G}$ so $\boldsymbol{a}_j = \boldsymbol{g}_j$. From (3) and (7), we obtain the SINR for a single user as

$$SINR_j = \frac{P_t\|\boldsymbol{h}_j\|^4\nu_j^2}{P_t\nu_j\sum_{k=1,k\neq j}^{K}|\boldsymbol{h}_j^H\boldsymbol{h}_k|^2\nu_k + \|\boldsymbol{h}_j\|^2\nu_j}. \tag{8}$$

Conditioned on $\boldsymbol{h}_j$, we define a new RV $\tilde{g_k}$ such that $\tilde{g_k} = \frac{|\boldsymbol{h}_j^H\boldsymbol{h}_k|}{\|\boldsymbol{h}_j\|}$. $\tilde{g_k}$ is a Gaussian RV with zero mean and unit variance that is independent of $\boldsymbol{h}_j$. Therefore, $\tilde{g_k} \sim \mathcal{CN}(0,1)$. From (8), the SINR is then given by

$$SINR_j = \frac{P_t\|\boldsymbol{h}_j\|^2\nu_j}{P_t\sum_{k=1,k\neq j}^{K}|\tilde{g_k}|^2\nu_k + 1}. \tag{9}$$

The numerator in (9) is the SNR, $Z$, of a single user at the BS. For notational simplicity, we omit the subscripts in the expression of $Z$. Therefore

$$Z = P_t\ \nu\sum_{i=1}^{M}|h_i|^2 := P_t\ \nu\ \gamma, \tag{10}$$

where $\gamma \sim \Gamma(M,1)$ owing to the sum of independent and identically distributed (i.i.d.) exponential RVs each having a unit mean. From (10), it is evident that the SNR follows a gamma-lognormal product distribution. Since $P_t$ is a constant, we neglect it in the PDF expression of gamma-lognormal product distribution. The PDF of the product of gamma and lognormal RVs is then given by

$$\begin{aligned} P_Z(z) = \frac{\xi z^{M-1}}{(M-1)!\ \sigma_{(dB)}\sqrt{2\pi}}\int_0^\infty \frac{\exp\left(-z/\nu\right)}{\nu^{(M+1)}} \\ \times \exp\left(\frac{-\left(\xi\log_e\nu - \mu_{(dB)}\right)^2}{2\sigma^2_{(dB)}}\right)d\nu, \end{aligned} \tag{11}$$

where $\xi = 10/\log_e 10$ is a scaling constant. From (11) it can be noticed that the SNR does not exist in a closed-form. The product distribution in (11) is approximated by a new lognormal RV $Y$. The parameters of RV $Y$ are then used to calculate the probability of outage, $\mathcal{O}$, for a single user as

$$\mathcal{O} = \mathbb{P}\left\{Z \leq \tau\right\} = Q\left(\frac{\mu_Y - 10\log_{10}\tau}{\sigma_Y}\right), \tag{12}$$

where Q-function gives the tail probability; $Q(x) = \frac{1}{\sqrt{2\pi}}\int_x^\infty \exp\left(\frac{-y^2}{2}\right)dy$, and $\mu_Y$ and $\sigma_Y$ are the mean and standard deviation, in dB, associated with the approximating RV $Y$, respectively, and $\tau$ is the modulation dependent threshold.

## III. Lognormal Approximation of SNR

In this section, we propose two methods to approximate the SNR (gamma-lognormal product distribution) by another lognormal RV. As the lognormal distribution is completely characterized by two parameters, namely the $mean$ and $variance$ of the associated Gaussian RV, hence the product distribution can be approximated by the lognormal distribution by finding the mean and variance of the Gaussian RV associated with the approximating lognormal RV.

### A. Moment Matching Method

In this method, the first and second central moments of the Gaussian RV $X_1$ associated with the approximating lognormal RV, $Y_1 = 10^{0.1X_1}$, are equated with the corresponding moments of the product RVs. The mean, $\mu_{X_1}$, associated with the approximating lognormal distribution is given by

$$
\begin{aligned}
\mu_{X_{1_{(dB)}}} &= \mathbb{E}\ \{10\log_{10} Z\} \\
&\overset{(a)}{=} \frac{\xi}{\sigma_{(dB)}\sqrt{2\pi}\,(M-1)\,!}\int_0^\infty\int_0^\infty (10\log_{10} Z)\frac{z^{M-1}}{\nu^{M+1}} \\
&\quad \times \exp\left(\frac{-z}{\nu}\right)\exp\left(-\frac{\left(\xi\ln\nu-\mu_{(dB)}\right)^2}{2\sigma^2_{(dB)}}\right)d\nu dz \\
&\overset{(b)}{=} \frac{\xi^2}{\sigma_{(dB)}\sqrt{2\pi}}\int_0^\infty \frac{1}{\nu}\left\{\psi(M)+\ln(\nu)\right\} \\
&\quad \times \exp\left(-\frac{\left(\xi\ln\nu-\mu_{(dB)}\right)^2}{2\sigma^2_{(dB)}}\right)\ d\nu \\
&\overset{(c)}{=} \xi\psi(M)+\mu_{(dB)},
\end{aligned}
\tag{13}
$$

where $\mathbb{E}$ is the expectation operator, (a) follows from (11), (b) follows after solving the inner integral with respect to $z$, (c) follows after substituting $\xi\ln\nu = z$ in (b) and then performing considerable algebraic manipulation, and $\psi(M) = -0.5772 + \sum_{k=1}^{M-1}\frac{1}{k}$.

The variance of $X_1$ is calculated from its second moment. The derivation of the second moment of $X_1$ follows similar steps as that of $\mu_{X_{1_{(dB)}}}$ and is given as

$$
\begin{aligned}
\mathbb{E}\left\{(10\log_{10} Z)^2\right\} &= \xi^2\left\{\psi(M)\right\}^2 + \xi^2\zeta\left(2,M\right) \\
&\quad + \mu^2_{(dB)} + \sigma^2_{(dB)} + 2\xi\psi\left(M\right)\mu_{(dB)},
\end{aligned}
\tag{14}
$$

where $\zeta(2,M) = \sum_{k=0}^{\infty}\frac{1}{(M+k)^2}$, is the Riemann-zeta function. The variance $\sigma^2_{X_{1_{(dB)}}}$ is then given as

$$
\begin{aligned}
\sigma^2_{X_1} &= \mathbb{E}\{(10\log_{10} Z)^2\} - \left(\mathbb{E}\{10\log_{10} Z\}\right)^2 \\
&\triangleq \sigma^2_{(dB)} + \xi^2\zeta(2,M).
\end{aligned}
\tag{15}
$$

The SNR can now be approximated by $Y_1 = 10^{0.1X_1}$ where $X_1 \sim \mathcal{N}(\mu_{X_1}, \sigma^2_{X_1})$ and $\mu_{X_1}$ and $\sigma_{X_1}$ are in dB.

### *B. MGF-based Method*

In this method, the MGFs of the approximating lognormal RV, $Y_2$, and the product RVs are equated to find the parameters $\mu_{X_2}$ and $\sigma^2_{X_2}$of $Y_2 = 10^{0.1X_2}$. However, the MGFs of both the lognormal and the product RVs do not exist in closed-form but they can be computed numerically by applying Gauss-Hermite integration. The MGF of $Y_2$ is given as

$$
\Psi_{Y_2}(s) = \int_0^\infty \exp(-sy)P_{Y_2}(y)\ dy,
\tag{16}
$$

where $P_{Y_2}(y) = \frac{\xi}{y\sigma_{X_2}\sqrt{2\pi}}\exp\left(\frac{-\left(\xi\log_e y-\mu_{X_2}\right)^2}{2\sigma^2_{X_2}}\right)$ is the lognormal PDF. Substituting $p = \frac{\xi\log_e y-\mu_{X_2}}{\sqrt{2}\sigma_{X_2}}$ in $P_{Y_2}(y)$, (16) can be rewritten as

$$
\begin{aligned}
\Psi_{Y_2}(s) &= \int_{-\infty}^{\infty}\frac{1}{\sqrt{\pi}}\exp\left(-p^2\right) \\
&\quad \times \exp\left[-s\exp\left(\frac{\sqrt{2}p\sigma_{X_2}+\mu_{X_2}}{\xi}\right)\right]dp.
\end{aligned}
\tag{17}
$$

Equation (17) takes the form of a Hermite polynomial, thus applying Gauss-Hermite integration to (17) results in

$$
\begin{aligned}
\Psi_{Y_2}(s;\mu_{X_2},\sigma_{X_2}) &= \sum_{t=1}^{T}\frac{w_t}{\sqrt{\pi}} \\
&\quad \times \exp\left[-s\exp\left(\frac{\sqrt{2}a_t\sigma_{X_2}+\mu_{X_2}}{\xi}\right)\right],
\end{aligned}
\tag{18}
$$

where $a_t$ are the roots (abscissas) of the Hermite Polynomial, $w_t$ are the corresponding weights and $T$ is the Hermite integration order. A higher value of $T$ corresponds to greater accuracy. The MGF of SNR is given by

$$
\begin{aligned}
\Psi_Z(s) &= \frac{\xi}{\sigma_{(dB)}\sqrt{2\pi}\,(M-1)\,!}\int_0^\infty\int_0^\infty \frac{z^{M-1}}{\nu^{M+1}}\exp\left(-sz\right) \\
&\quad \times \exp\left(\frac{-z}{\nu}\right)\exp\left(\frac{-\left(\xi\log_e\nu-\mu_{(dB)}\right)^2}{2\sigma^2_{(dB)}}\right)d\nu dz \\
&\overset{(a)}{=} \frac{\xi}{\sigma_{(dB)}\sqrt{2\pi}}\int_0^\infty \frac{1}{\nu}\frac{1}{\left(1+s\nu\right)^M} \\
&\quad \times \exp\left(\frac{-\left(\xi\log_e\nu-\mu_{(dB)}\right)^2}{2\sigma^2_{(dB)}}\right)d\nu \\
&\overset{(b)}{=} \frac{1}{\sqrt{\pi}}\int_{-\infty}^{\infty}\frac{\exp\left(-q^2\right)}{\left[1+s\exp\left(\frac{q\sqrt{2}\sigma_{(dB)}+\mu_{(dB)}}{\xi}\right)\right]^M}\ dq \\
&\overset{(c)}{=} \frac{1}{\sqrt{\pi}}\sum_{t=1}^{T}\frac{w_t}{\left[1+s\exp\left(\frac{a_t\sqrt{2}\sigma_{(dB)}+\mu_{(dB)}}{\xi}\right)\right]^M},
\end{aligned}
\tag{19}
$$

where (a) follows by solving the inner integral with respect to $z$, (b) follows by substituting $q = \frac{\xi\ln\nu-\mu_{(dB)}}{\sigma_{(dB)}\sqrt{2}}$ in (a) and simplifying the expression, and (c) results by applying Gauss-Hermite integration to (b).

The parameters of the approximate lognormal RV can then be calculated by equating (18) and (19) at two distinct positive and real values of $s$, identified by $s_1$ and $s_2$. This forms a system of two non-linear equations given by

$$
\begin{aligned}
&\sum_{t=1}^{T}\frac{w_t}{\sqrt{\pi}}\exp\left[-s_i\exp\left(\frac{\sqrt{2}\sigma_{X_2}a_t+\mu_{X_2}}{\xi}\right)\right] \\
&\quad = \Psi_Z(s_i;\mu_{(dB)},\sigma_{(dB)}), \qquad \text{for } i\text{=1 and 2.}
\end{aligned}
\tag{20}
$$

The non-linear system of equations in (20) can be solved for $\mu_{X_2}$ and $\sigma_{X_2}$using a numerical routine. The values of $s_1$ and $s_2$ have significant effect on the performance of this approximation method. It is found that the optimal results are achieved when $s_1$, $s_2 \in (0,1]$. Multiplication by $P_t$ as in (10) simply shifts $\mu_{X_1}$ and $\mu_{X_2}$.Therefore

$$
Z \sim Log\mathcal{N}(\mu_X + \xi\log_e P_t, \sigma^2_X),
\tag{21}
$$

where $\mu_X$ and $\sigma^2_X$ can be calculated by either of the methods explained above.

## IV. Lognormal Approximation of SINR

Approximating the SINR by a lognormal RV is also based on the two above mentioned approximating methods. The summation in the denominator of (9) involves a product of exponential and lognormal RVs. The distribution of the product of these RVs also does not exist in a closed-form but can be approximated another lognormal RV, $W \sim \text{Log-}\mathcal{N}(\mu_a, \sigma_a^2)$. Since gamma RV is a sum of i.i.d. exponential RVs, substituting $M = 1$ in (13) and (15) gives the parameters of $W$ through the moment-matching technique. The sum of $K$ independent approximating lognormal RVs, $W$, can then be approximated by yet another lognormal RV by the MGF method [7].

Alternatively, substituting $M = 1$ in (19) gives the MGF of the product of exponential and lognormal RVs. This MGF is the same as the MGF of a Suzuki RV given in [7]. In [7], the authors have proposed an MGF-based method to approximate the sum of independent Suzuki RVs by a new lognormal RV. We use the same proposed method to serve our purpose and approximate the sum of product of exponential and lognormal RVs by a new RV, $R \sim \text{Log-}\mathcal{N}\left(\mu_b, \sigma_b^2\right)$.

Addition of 1 to the sum of exponential-lognormal RVs in (9) simply adds unity to the expected value of RV $R$. The SINR of the $j$th user in (9) can now be expressed as a ratio of two independent lognormal RVs, $Z$ and $R$.

$$SINR_j = \frac{Z}{R} := \frac{Log\mathcal{N}(\mu_X + \xi \log_e P_t, \sigma_X^2)}{Log\mathcal{N}(\mu_b + \xi \log_e P_t, \sigma_b^2)}. \quad (22)$$

The ratio of two lognormals is again a lognormal RV. Therefore

$$SINR_j \sim Log\mathcal{N}(\mu_X - \mu_b, \sigma_X^2 + \sigma_b^2). \quad (23)$$

## V. Numerical Results

In this section, we plot the cumulative distribution function (CDF) and the complementary CDF (CCDF) to verify the accuracy of the proposed lognormal approximation of SNR and SINR. We also plot the outage probability for a multi-user scenario under different channel conditions.

### A. SNR Approximation

Fig. 1 shows the CDF and the CCDF of SNR considering 500 BS antennas. The curves are obtained using Monte-Carlo simulations and compared with the two prosposed lognormal approximation methods. Optimal values of $s_1$ = 0.001 and $s_2$ = 0.005 have been chosen. Both the proposed methods approximate the SNR with a good accuracy. It can be seen, however, that the CCDF is approximated with a greater accuracy as compared to the CDF for ($s_1$,$s_2$) = (0.001, 0.005). Greater accuracy in approximating the CCDF implies that the tail of SNR PDF is approximated precisely. The tail of SNR PDF is particularly important in calculating the outage probability. The mean absolute error (MAE) of both the proposed approximation methods is of the order of $10^{-8}$. While calculating the outage probability, we need an approximation of SNR PDF with the least MAE.

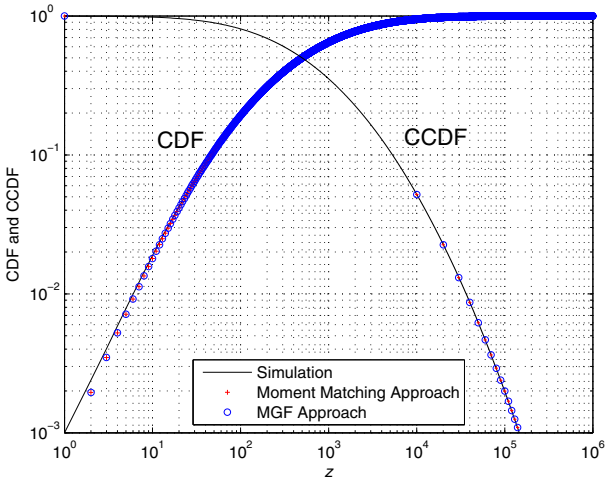


Fig. 1: Comparison of accuracy of CDF and CCDF of the two proposed methods for 500 BS antennas ($\mu_{dB} = 0$ and $\sigma_{dB} = 8$).

The lognormal approximation of SINR gives similar results. Due to space constraint and to avoid repetition, we omit the CDF and CCDF plots of SINR.

### B. Outage Probability

From (12) and (23), the outage in a multi-user scenario is given by

$$\mathcal{O} = \mathbb{P}\{SINR \leq \tau\} = Q\left(\frac{\mu_X - \mu_b - 10\log_{10}\tau}{\sqrt{\sigma_X^2 + \sigma_b^2}}\right). \quad (24)$$

Before discussing the results for outage probability, we define a new term, SNR margin, $\rho$. The SNR margin, $\rho$, is interpreted as the normalized transmit SNR of a user and is given by $\rho = \frac{P_t}{\tau}$, where $\tau$ is the modulation dependent threshold.

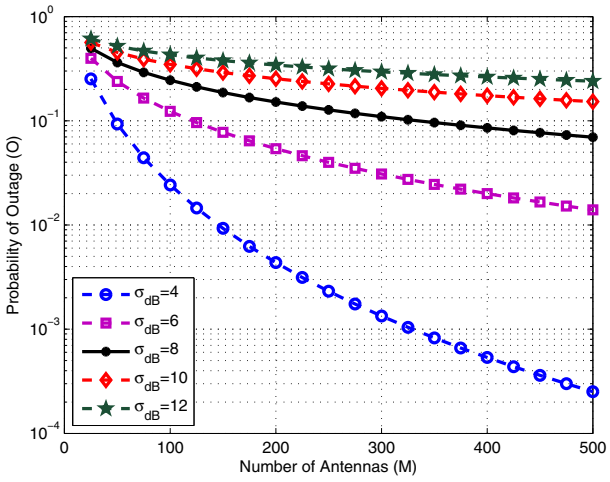


Fig. 2: Probability of outage with 10 users. All users experience same shadowing ($\mu_{dB} = 0$ and $\rho = 10$ dB).

Fig. 2 shows that the outage decreases with an increase in the number of antennas. However, the decrease in outage is more prominent for a lightly-shadowed system as compared to a heavily-shadowed system because unlike small-scale fading, shadowing does not average out by increasing number of the antennas. Fig. 2 quantifies the effect of shadowing on outage.

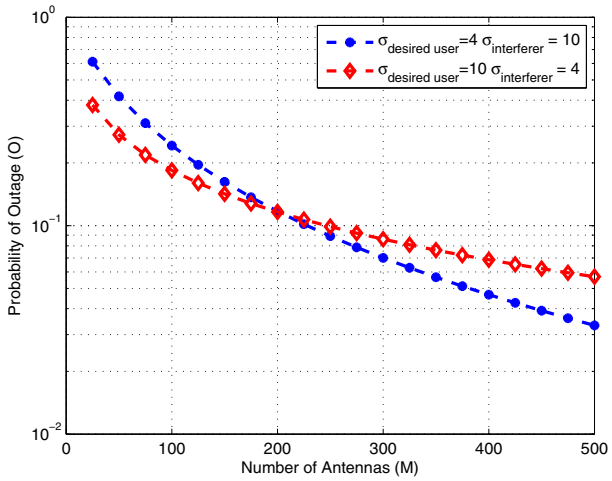


Fig. 3: Probability of outage in two different scenarios. ($\mu_{dB} = 0, \rho = 10$ dB and $K = 10$).

Fig. 3 plots the outage probability for two different scenarios. In the first scenario, the desired user suffers light shadowing and the interferers are severely shadowed, whereas it is vice versa in the other scenario. It can be seen that when the desired user is severely shadowed, the user experiences less outage for lesser number of antennas. This is because the shadowing phenomenon models the fluctuations in the received power around a certain mean; the average SINR defines the mean which is a function of number of antennas. These fluctuations become large when $\sigma_{(dB)}$ of shadowing is increased. Therefore, on the average, the received power crosses a set threshold more often and the user experiences less outage. For the channel conditions of Fig. 3, one can get a favourable shadowing outcome at lesser number of antennas, which eventually reduces the outage probability. This is contrary to the case where the channel consists only of small-scale fading and only an increase in the number of BS antennas averages out the fading effect and reduces the outage probability. In Fig. 3, both the scenarios have the same outage probability at 200 BS antennas. This gives an estimate of the shadow margin that needs to be kept at the user side. For different channel conditions, the shadow margin will be different.

Fig. 4 shows the diminishing trend of reduction in the outage as $M$ is increased. The reduction in outage for a specific $\rho$ is more prominent when we increase $M$ from 50 to 100 as compared to the case when we increase $M$ from 400 to 500. This is because the diversity gain of the system does not increase linearly with the increase in number of antennas.

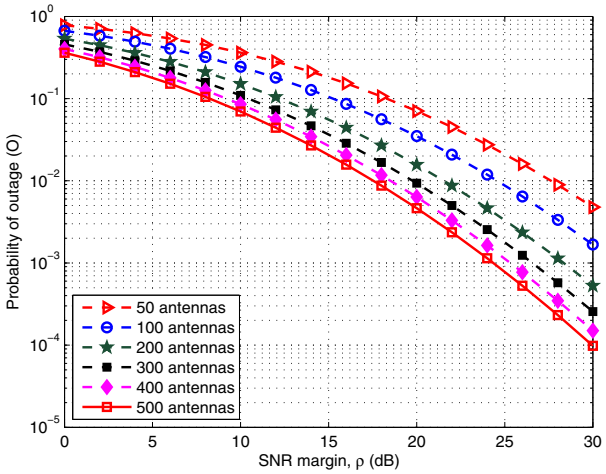


Fig. 4: Probability of outage with 10 users. All users experience same shadowing ($\mu_{dB} = 0, \sigma_{dB} = 8$ dB and $K = 10$).

Moreover, there is a trade-off between the SNR margin and the number of antennas. If either of the quantities is reduced, then the other quantity needs to be increased in order to maintain a specific quality of service, which is the outage probability in this case.

## VI. Conclusion

We have approximated the PDF of SINR for an MRC receiver with a single lognormal RV under composite shadowing-fading environment, assuming perfect CSI. Closed-form expression for the outage probability has been provided. We have quantified the effects of shadowing on the outage of multi-user massive MIMO systems. The outage analysis asserts that shadowing does not average out by increasing the number of antennas. As a future work, we intend to include the effects of pilot contamination, extend the proposed analysis to a multi-cell scenario and work with imperfect CSI.

## References


[1] T. L. Marzetta, "Noncooperative cellular wireless with unlimited numbers of base station antennas," *IEEE Trans. Wireless. Commun.,* vol. 9, no. 11, pp. 3590-3600, Nov. 2010.

[2] F. Rusek, D. Persson, B. K. Lau, E. G. Larsson, T. L. Marzetta, O. Edfors, and F. Tufvesson,"Scaling up MIMO: Opportunities and challenges with very large arrays," *IEEE Signal Process. Mag.,* vol. 30, pp. 40-60, Jan. 2013.

[3] H. Yang and T. L. Marzetta, "Performance of conjugate and zero-forcing beamforming in large-scale antenna systems," *IEEE J. Sel. Areas Commun.,* vol. 31, no. 2, pp. 172-179, Feb. 2013.

[4] E. Larsson, F. Tufvesson, O. Edfors, T. Marzetta, "Massive MIMO for next generation wireless systems," *IEEE Commun. Mag*., vol. 52, no. 2, pp.186-195, Feb. 2014.

[5] H. Q. Ngo, E. G. Larsson, T. L. Marzetta, "Energy and spectral efficiency of very large multiuser MIMO systems," *IEEE Trans. Wireless Commun.*, vol. 61, no. 4, pp. 1436-1449, April 2013.

[6] C. Studer, E. G. Larsson, "PAR-aware large-scale multi-user MIMO-OFDM downlink," *IEEE J. Sel. Areas Commun*., vol. 31, no. 2, pp. 303-313, Feb. 2013.

[7] N. B. Mehta, J. Wu, A. F. Molisch, and J. Zhang, "Approximating a sum of random variables with a lognormal," *IEEE Trans. Wireless Commun.,* vol. 6, pp. 2690-2699, July 2007.